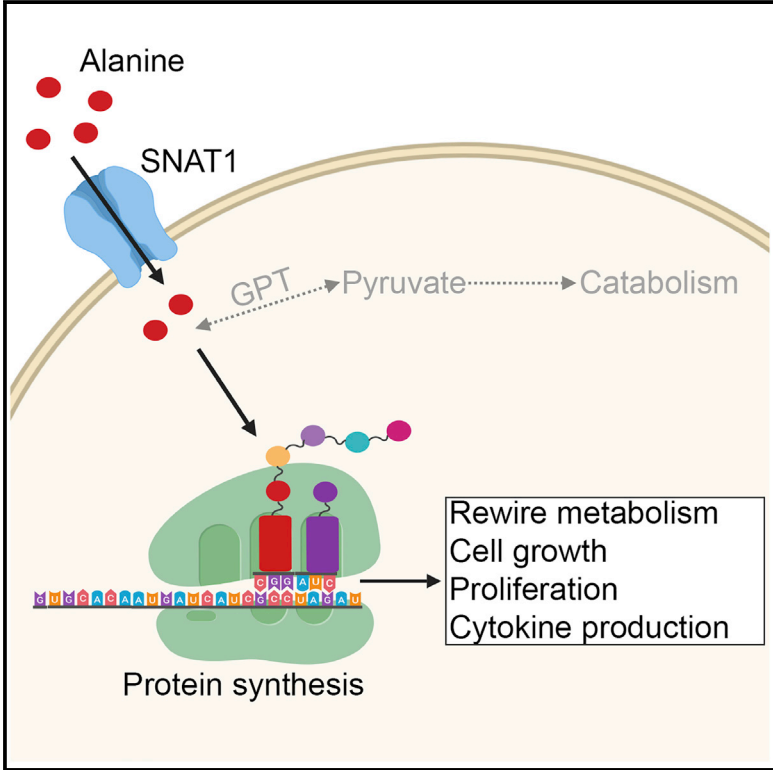


T Cell Activation Depends on Extracellular Alanine

Graphical Abstract



Authors

Noga Ron-Harel,
Jonathan M. Ghergurovich,
Giulia Notarangelo, ..., Arlene H. Sharpe,
Joshua D. Rabinowitz, Marcia C. Haigis

Correspondence

marcia_haigis@hms.harvard.edu (M.C.H.),
Arlene_Sharpe@hms.harvard.edu (A.H.S.),
josh@Princeton.EDU (J.D.R.),
nogaronharel@technion.ac.il (N.R.-H.)

In Brief

In health, T lymphocytes are in a resting state. However, stimulation with their cognate antigen induces massive growth and proliferation. Ron-Harel et al. demonstrate that T cells rely on extracellular alanine for activation. Consumed alanine is used primarily for protein synthesis, and alanine deprivation inhibits T cell metabolism and effector functions.

Highlights

- Alanine is an essential amino acid for T cells to exit quiescence
- Alanine deprivation during early activation leads to functional impairment
- T cells do not catabolize alanine during early activation
- Extracellular alanine supports protein synthesis



T Cell Activation Depends on Extracellular Alanine

Noga Ron-Harel,^{1,9,10,*} Jonathan M. Ghergurovich,^{2,3,9} Giulia Notarangelo,^{1,9} Martin W. LaFleur,⁴ Yoshiki Tsubosaka,^{1,5} Arlene H. Sharpe,^{4,6,7,*} Joshua D. Rabinowitz,^{2,8,*} and Marcia C. Haigis^{1,11,*}

¹Department of Cell Biology, Blavatnik Institute, Harvard Medical School, Boston, MA 02115, USA

²The Lewis-Sigler Institute for Integrative Genomics, Princeton University, Princeton, NJ 08544, USA

³Department of Molecular Biology, Princeton University, Princeton, NJ 08544, USA

⁴Department of Immunology, Blavatnik Institute, Harvard Medical School, Boston, MA 02115, USA

⁵Pharmacology Research Department, Teijin Institute for Bio-Medical Research, Teijin Pharma Limited, Tokyo 1918512, Japan

⁶Evergrande Center for Immunologic Diseases, Harvard Medical School and Brigham and Women's Hospital, Boston, MA 02115, USA

⁷Department of Pathology, Brigham and Women's Hospital, Boston, MA 02115, USA

⁸Department of Chemistry, Princeton University, Princeton, NJ 08544, USA

⁹These authors contributed equally

¹⁰Present address: Faculty of Biology, Technion, Haifa 3200003, Israel

¹¹Lead Contact

*Correspondence: nogaronharel@technion.ac.il (N.R.-H.), Arlene_Sharpe@hms.harvard.edu (A.H.S.), josh@Princeton.EDU (J.D.R.),

marcia_haigis@hms.harvard.edu (M.C.H.)

<https://doi.org/10.1016/j.celrep.2019.08.034>

SUMMARY

T cell stimulation is metabolically demanding. To exit quiescence, T cells rely on environmental nutrients, including glucose and the amino acids glutamine, leucine, serine, and arginine. The expression of transporters for these nutrients is tightly regulated and required for T cell activation. In contrast to these amino acids, which are essential or require multi-step biosynthesis, alanine can be made from pyruvate by a single transamination. Here, we show that extracellular alanine is nevertheless required for efficient exit from quiescence during naive T cell activation and memory T cell restimulation. Alanine deprivation leads to metabolic and functional impairments. Mechanistically, this vulnerability reflects the low expression of alanine aminotransferase, the enzyme required for interconverting pyruvate and alanine, whereas activated T cells instead induce alanine transporters. Stable isotope tracing reveals that alanine is not catabolized but instead supports protein synthesis. Thus, T cells depend on exogenous alanine for protein synthesis and normal activation.

INTRODUCTION

In health, naive and memory T cells are retained in a quiescent state. In response to pathogen exposure, these cells quickly exit quiescence and enter a cycle of rapid cell growth and robust proliferation to generate large numbers of effector cells to fight off threats and restore homeostasis. The transition from quiescence to activation is driven by metabolic adaptation of these cells to meet their changing needs. With activation, glycolysis is highly induced, and glucose-derived carbon fuels multiple

synthetic pathways, including the pentose phosphate and serine biosynthetic pathways, both of which contribute to *de novo* generation of nucleotides. In parallel, glucose-derived pyruvate feeds into the tricarboxylic acid (TCA) cycle, where it supplies a carbon source for lipid synthesis and electrons for ATP synthesis by the generation of citrate (Berod et al., 2014) and the electron transport chain, respectively.

To adequately fuel these metabolic pathways, which often share common resources, activated T cells rely on extracellular pools of precursor nutrients. For example, glutamine-derived carbon feeds into the TCA cycle to compensate for the export of citrate from the mitochondria to the cytosol, where it is used for fat synthesis (Berod et al., 2014). Although glutamine is not an essential amino acid and can, therefore, be synthesized by mammalian cells, successful T cell activation depends on access to extracellular glutamine and its uptake (Carr et al., 2010; Nakaya et al., 2014). Similarly, although serine can be synthesized from the glycolytic intermediate 3-phosphoglycerate, extracellular serine remains the primary carbon source for mitochondrial one-carbon metabolism, the main pathway in T cells for supplying one-carbon units for purine and thymidine biosynthesis (Ron-Harel et al., 2016). Accordingly, serine deprivation from the diet is sufficient to impair T cell proliferation and effector functions (Ma et al., 2017). These studies emphasize how T cells depend on extracellular nutrients, including nonessential amino acids, to meet their rapidly changing metabolic needs upon activation.

Controlling the uptake of these nutrients is a key mechanism for regulating T cell activation (Geiger et al., 2016; Patsoukis et al., 2015; Ramsay and Cantrell, 2015; Rodriguez et al., 2007; Rollings et al., 2018; Wieman et al., 2007; Wofford et al., 2008). In this study, building on work done nearly 40 years ago describing a role for alanine in supporting T cell activation (Rotter et al., 1979), we identify alanine as an extracellular nutrient critical for T cells to transition from quiescence to activation. Our findings show that the nonessential amino acid alanine is not synthesized by T cells during early activation. Instead, naive



T cells rely on extracellular alanine pools for their initial activation, and memory T cells need extracellular alanine for successful re-stimulation. Alanine deprivation negatively affects cell growth, proliferation and effector functions, and skews activation-induced metabolic reprogramming. Interestingly, in contrast to certain cancer cells that catabolize alanine (Sousa et al., 2016), T cells appear to exclusively use extracellular alanine for protein synthesis.

RESULTS

Extracellular Alanine Is Essential for Initial Activation of Naive T Cells

We discovered T cell reliance on extracellular alanine for activation while investigating why dialyzed serum inhibited the activation of T cells *in vitro*. To identify extracellular nutrients that are required for T cell activation, we utilized a well-established system for *ex vivo* stimulation. Sorted naive CD62L⁺CD25⁻CD44^{lo} CD4⁺ T cells were cultured with soluble anti-CD3 and antigen presenting cells (APCs) to stimulate the T cell receptor (TCR) and co-stimulatory signals required for proper activation (Figure 1A) in the presence of standard “complete” fetal bovine serum (cFBS) or dialyzed FBS (dFBS). As expected, T cell stimulation resulted in increased T cell size in cFBS. However, the increase in cell size was blunted in dFBS (Figure 1B). To assess changes in effector function, we quantified secreted cytokine levels in spent culture media after cells were activated and cultured for 72 h. The concentrations of the proinflammatory cytokines interleukin-17 (IL-17), interferon γ (IFN γ), and IL-6 were all significantly reduced in the spent media from cells activated in the presence of dFBS (Figure 1C). Moreover, cells cultured in dFBS media proliferated less in the 72 h following activation (Figure 1D). These findings suggest that at least one factor that is important for T cell stimulation is lost through FBS dialysis. To validate these findings in an orthogonal system, we stimulated sorted naive CD4⁺ T cells with plate-bound anti-CD3 and anti-CD28 (Figure S1A). As with APC-driven stimulation, culture in dFBS media impaired cell growth (Figure S1B) and proliferation (Figure S1C). Notably, alanine deprivation did not have a profound effect on the expression of early activation markers, as demonstrated with CD69 (Figure S1D). Because this simplified system proved suitable for *ex vivo* analysis of purified T cell cultures, it was used for all subsequent experiments.

Standard T cell culture media contains 10% serum. Reducing the cFBS portion to 2.5% (offsetting with 7.5% dFBS to maintain total serum concentration) led to no observable effect on post-activation proliferation. However, further dilution of the cFBS fraction caused a substantial delay in proliferation (Figure 1E). Our findings suggest that early T cell activation requires one or more components found in cFBS that are reduced by >75% by dialysis. To identify this unknown component(s), growth media (RPMI) prepared with either 10% cFBS or 10% dFBS was analyzed by liquid chromatography mass spectrometry (LC-MS) in negative ionization mode. Chromatographic separation was achieved by two approaches: reverse-phase ion-pairing chromatography (Figure 1F) and hydrophilic interaction liquid chromatography (HILIC) chromatography (Figure S1E), with metabolites identified based on exact mass and retention time

matched to authenticated standards. A set of 12 metabolites was independently identified by both LC-MS methods as being reduced by >75% in the dFBS media (Figure S1F).

To determine which of the identified metabolites is essential for early T cell activation, naive T cells were activated using media containing cFBS, dFBS, or dFBS supplemented with each of the 12 candidate metabolites. Cells were collected at 24 h post-activation for the analysis of cell growth by flow cytometry. Strikingly, only alanine supplementation effectively rescued cell growth in dFBS media (Figure 1G). Although dialysis depletes every amino acid from serum, alanine is the only one of the 20 proteogenic amino acids not present in commercial RPMI media. Thus, serum supplementation supplies all of the alanine present in growth media.

To further investigate the dependency of proper T cell activation on extracellular alanine, naive T cells were stimulated in media made with cFBS, dFBS, or dFBS + alanine (Figure S1G). Results were confirmed across four different lots of dFBS. The concentration of alanine for supplementation was selected based on its normal serum concentration in humans (140–580 μ M) and measurement of 1.5-mM alanine in pure FBS by using an isotopic internal standard (Figure 1H; Figure S1H), implying an alanine concentration in medium with 10% cFBS of 150 μ M. A total of 100- μ M alanine completely rescued activation-induced growth and proliferation (Figures 1I and 1J, respectively).

Alanine Is Not an Important Catabolic Substrate

T cell activation causes dramatic metabolic upregulation, including simultaneous increases in aerobic glycolysis and mitochondrial metabolism. Therefore, we hypothesized that alanine could be an essential source of pyruvate for feeding into the TCA cycle during early T cell activation (Figure 2A). To test the effect of alanine deprivation on metabolic reprogramming, naive T cells were stimulated using the different media conditions and collected at 24 h post-activation for analysis of metabolic activity (Figure 2B). Cellular alanine and metabolic intermediates in glycolysis, the pentose phosphate pathway, and the TCA cycle (Figure 2C) were lower in T cells activated in dFBS-only media compared to media supplemented with cFBS and were rescued by alanine supplementation. Consistent with these findings, at 24 h post-activation, extracellular acidification rate (ECAR; Figure 2D), mitochondrial basal respiration, and maximal respiratory capacity (Figures 2E–2G) were suppressed in T cells stimulated in dFBS media and rescued by alanine. Notably, the effect of alanine deprivation on metabolic reprogramming was not immediate, as at 9 h post-activation, which precedes most activation-induced protein synthesis, concentrations of cellular metabolites were similar in T cells activated with and without alanine (Figure S2A). Thus, the widespread metabolic reprogramming that arises from T cell activation is impaired in the absence of extracellular alanine.

To directly test the catabolic fate of alanine, we cultured T cells in dFBS media with two different isotopically labeled forms of alanine ([U-¹³C]-alanine or [¹⁵N]-alanine; Figure 3A). Transamination of [U-¹³C]-alanine will give rise to ([U-¹³C]-pyruvate), which can subsequently be reduced to lactate or oxidized to enter the TCA cycle, in both cases giving rise to ¹³C-labeled products.

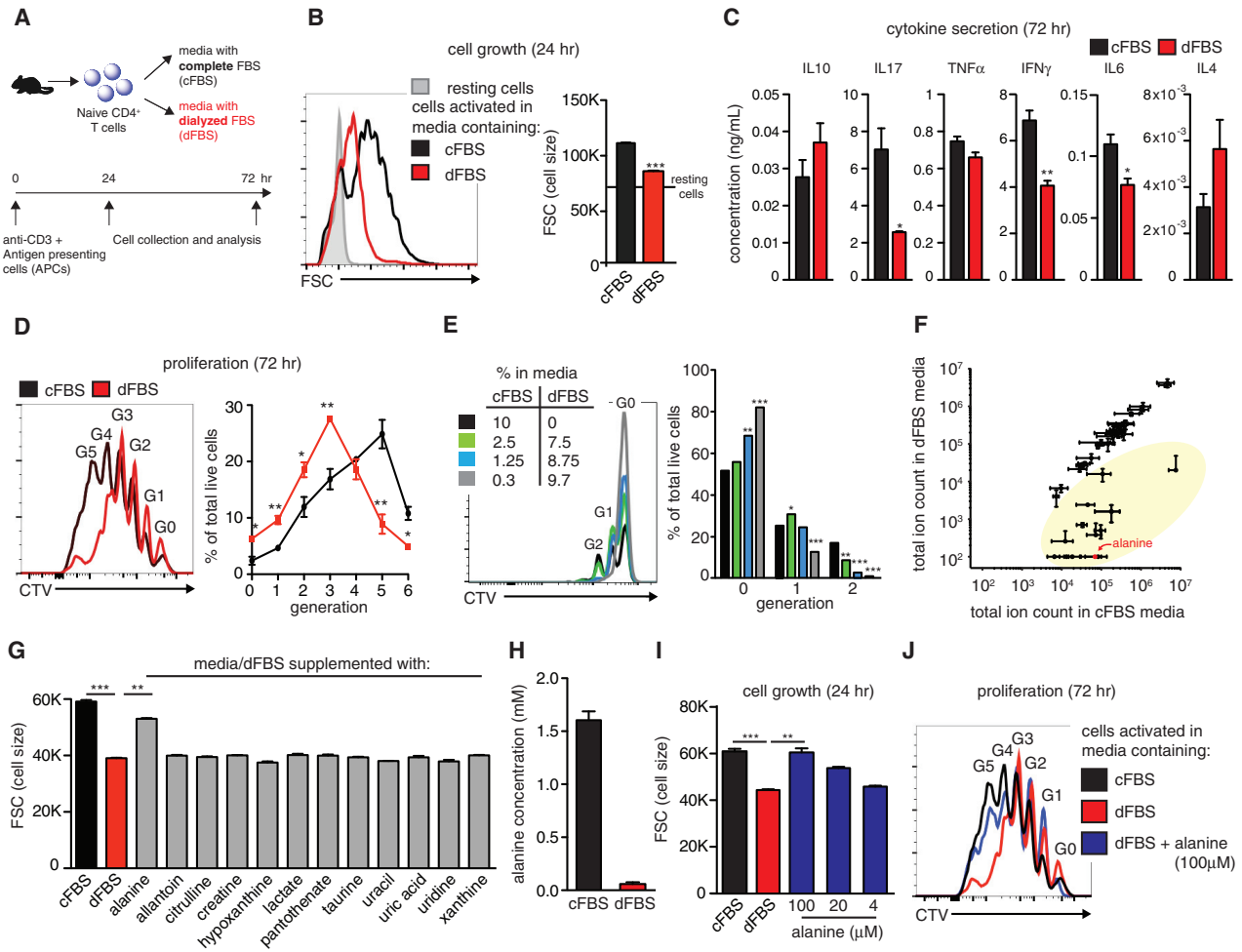


Figure 1. Alanine Deprivation Delays Early T Cell Activation

(A) Scheme of experimental design. Purified naive CD4⁺ T cells were activated *in vitro* in growth media containing 10% of either complete or dialyzed FBS (cFBS or dFBS, respectively).
 (B) A representative flow-cytometry plot and its quantitation, showing activation-induced growth in cell size.
 (C) Cytokine secretion into growth media was analyzed by flow cytometry at 72 h post-activation (n = 3).
 (D and E) Proliferation (number of cell divisions detected by dilution of CellTrace) was assessed in cells activated under conditions described in (A) (D) and in cells activated for 48 h in media prepared with various fractions of cFBS and dFBS (n = 4) (E).
 (F) Growth media prepared with either 10% cFBS or dFBS was analyzed by LC-MS (using reverse-phase chromatography; n = 2). Metabolites highlighted in yellow have reduced concentrations in dFBS media.
 (G) Rescue cell growth experiments at 24 h post-activation using media supplemented with selected metabolites absent in dFBS media (at final concentrations of 100 μM; n = 3).
 (H) Calculated alanine concentration in cFBS and dFBS as determined by LC-MS by using an internal standard ([¹⁵N]-alanine, n = 3 for three different standard concentrations).
 (I) Activation-induced growth in cell size in different media conditions (n = 3).
 (J) Proliferation in different media conditions with alanine supplementation (n = 3).
 Results are mean ± SEM. *p < 0.05, **p < 0.01, ***p < 0.001 (Student's t test comparing each of the conditions to dFBS media). All results are representatives of two or more independent experiments.

Similarly, transamination of [¹⁵N]-alanine will give rise to [¹⁵N]-glutamate (Figure 3B). Interestingly, no ¹³C-labeling from alanine was detected in pyruvate or lactate, TCA cycle intermediates, or glutamate. Indeed, the only substantially ¹³C-labeled aqueous metabolites detected in these tracing experiments were alanine itself and its acetylated derivative (N-acetyl-L-alanine) (Figure 3C; Figure S2B). As positive controls, we detected extensive labeling

of TCA cycle intermediates and glutamate from both pyruvate (Figure 3C; Figure S2B) and glutamine (Figures S2C and S2D). Although a significant amount of alanine is labeled from ¹³C-pyruvate, this likely arises from exaggerated transaminase activity driven by the artificially high concentration of media pyruvate (1 mM), which is not present in the media for any other condition. To rule out the possibility that alanine catabolism is defective

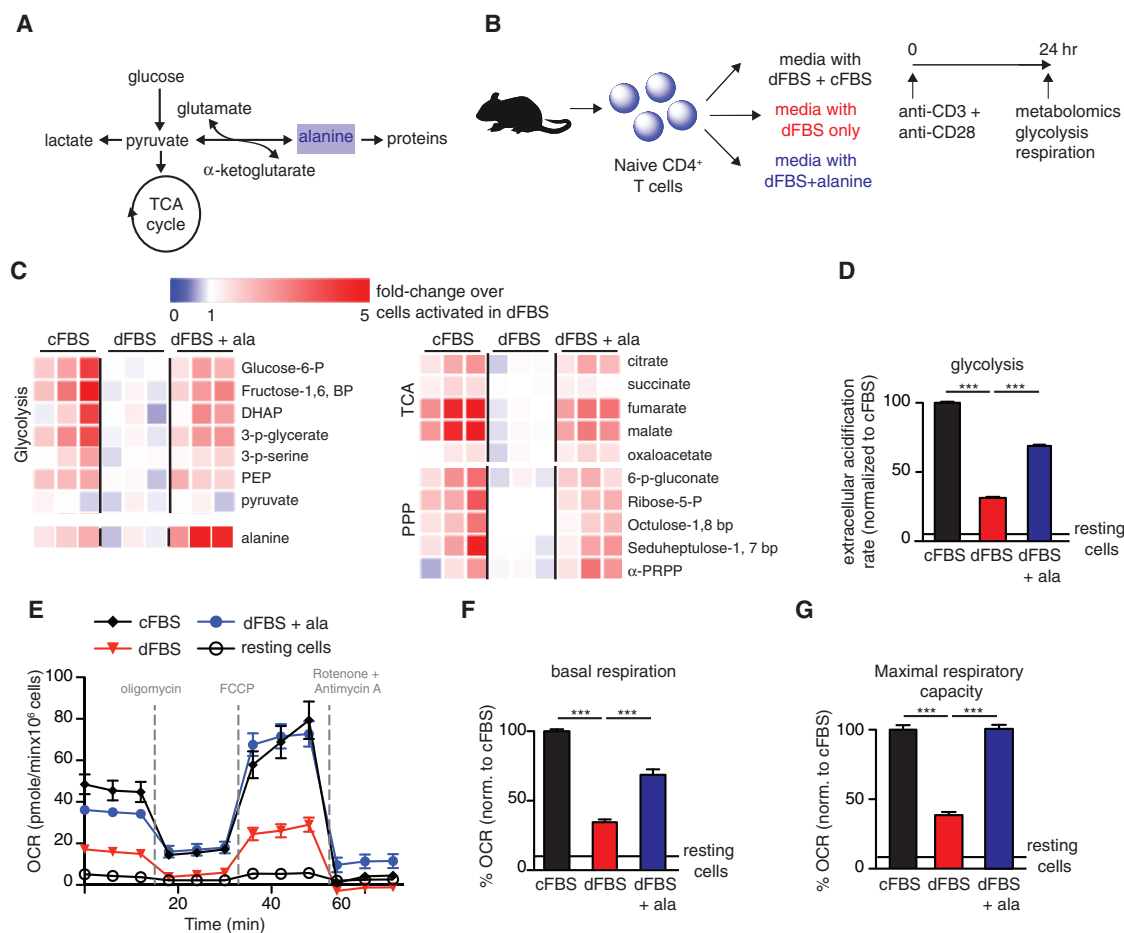


Figure 2. Alanine Deprivation Skews T Cell Metabolism

(A) Schematic showing metabolic fates of alanine in T cells.

(B) Experimental design for evaluating metabolic impact of alanine in T cell activation. Media were supplemented with 10% of either dFBS, a mix of cFBS/dFBS (1:3), or dFBS with 100 μM alanine.

(C) Changes in metabolite abundance in activated CD4⁺ T cells, normalized to levels in cells activated in dFBS.

(D–G) Evaluation of T cell metabolic function by the Seahorse extracellular flux analyzer (n = 8–10 replicates/condition): (D) extracellular acidification rate under blockade of mitochondrial respiration (measure of maximal glycolytic capacity); (E) changes in oxygen consumption rate (OCR) in activated T cells; (F) quantification of basal respiration; and (G) OCR following mitochondrial uncoupling (maximal respiratory capacity).

Results are mean ± SEM of at least 2 individual experiments. ***p < 0.001 (Student's t test comparing each of the conditions to dFBS media).

selectively in dFBS media, we performed alanine tracing experiments in cFBS media. Again, we found no evidence of alanine catabolism by the recently activated T cells (Figure S2E). The lack of pyruvate and TCA intermediate labeling from ¹³C-alanine (at concentrations that fully rescue activation) implies the absence of meaningful alanine to pyruvate transaminase activity. We, therefore, concluded that T cells do not substantially catabolize alanine, and the decreased levels of central carbon metabolites in cells deprived of alanine were mediated, at least in part, by a reduction in glucose uptake (Figures S2F and S2G).

T Cells Are Low in Alanine Transaminase, the Enzyme Required for Both Alanine Catabolism and Synthesis

Alanine can be synthesized from glucose through pyruvate transamination by the enzyme alanine aminotransferase, also known as glutamate-pyruvate transaminase (GPT; Figure 3C).

To examine the extent of alanine production, naive T cells were activated in standard cFBS media, supplemented with uniformly labeled glucose [U-¹³C-glc]. At 5 h post-activation, only 1%–2% of cellular alanine was labeled (Figure S3A). Thus, newly synthesized alanine is not a major source of alanine during early activation. Interestingly, in an independent experiment, we observed a small amount of alanine accumulation in the media over time (Figure S3B). However, it is unclear if this apparent excretion of *de novo* alanine is deliberate or is an artifact arising from the diffusion of intracellular alanine into the alanine-free (because dFBS lacks alanine) culture media. In addition to alanine synthesis, the major fates of pyruvate are oxidation to acetyl-coenzyme A (CoA) by pyruvate dehydrogenase (PDH) and reduction to lactate by lactate dehydrogenase (LDH) (Figure 3C). qPCR analysis showed massive upregulation of genes in the PDH and LDH complexes with T cell activation but a slight suppression or low

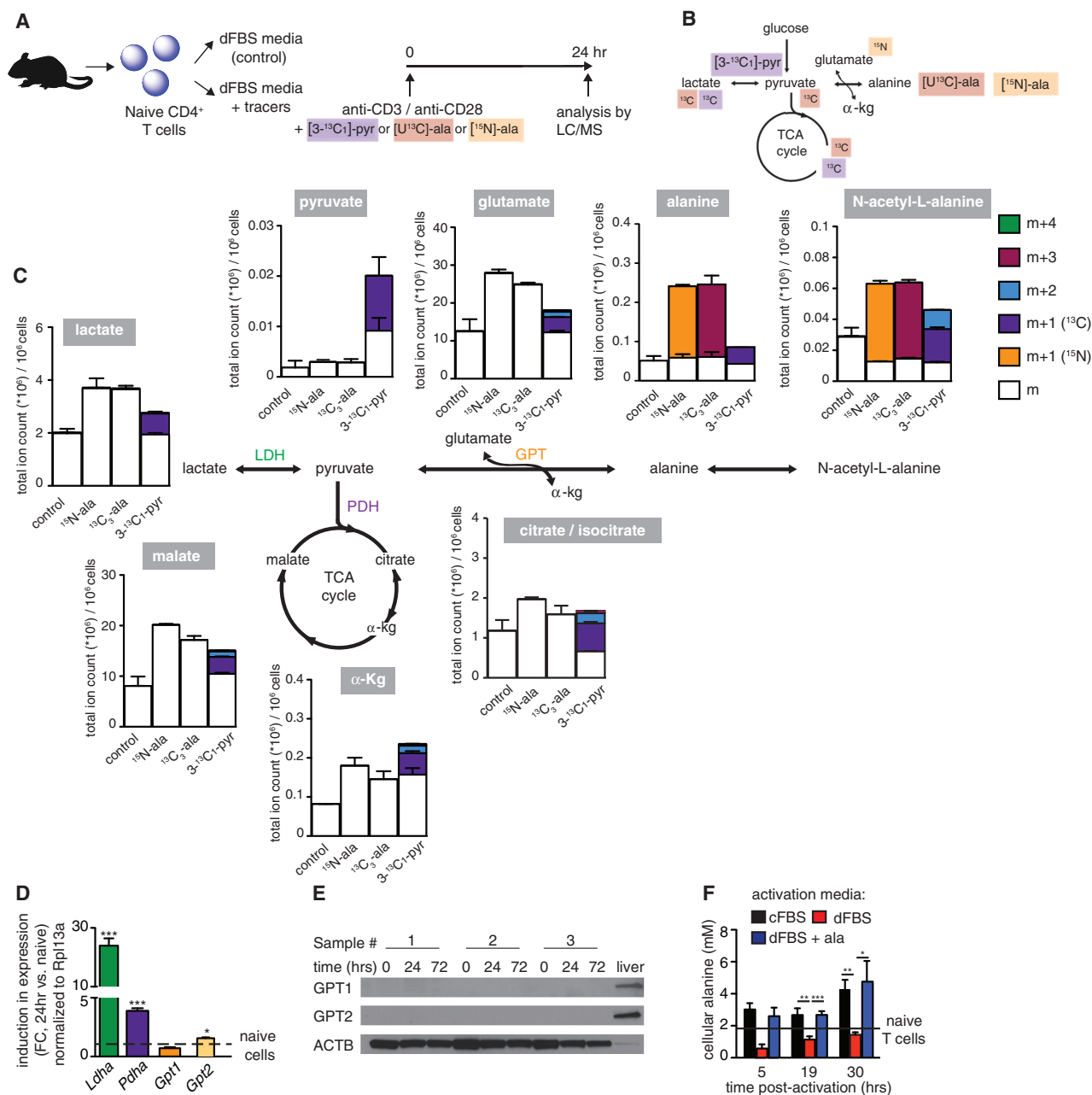


Figure 3. Activated T Cells Do Not Catabolize Alanine

(A) Experimental design for tracing the catabolic fate of alanine in activated T cells. Media were supplemented with dFBS and either of the following isotopic tracers: [3-¹³C₁]-pyr (1mM), [U-¹³C]-ala (100 μM), or [¹⁵N]-ala (100 μM).

(B) Schematic of anticipated incorporation of the tracers into relevant metabolic pathways.

(C) Graphs summarize the normalized total ion counts of different isotopomers of representative metabolites in T cells activated in the presence of different tracers (A) (n = 2). Isotope labeling data have been corrected for ¹³C natural abundance. LDH, lactate dehydrogenase; PDH, pyruvate dehydrogenase; GPT, glutamate-pyruvate transaminase (also known as alanine transaminase).

(D) Expression of LDH (*Ldha*) and PDH (*Pdha*) complex subunits and of GPT isoforms (*Gpt1* and *Gpt2*) were measured by qPCR. Fold-change in induced expression (activated versus naive T cells) was normalized to Rpl13a (n = 3).

(E) Protein quantitation of GPT1 and GPT2 by western blot, comparing naive and activated T cells. Samples of mouse liver were used as positive control.

(F) Cellular alanine concentration determined by LC-MS by using an internal standard ([U-¹³C]-alanine) (n = 3). Results are representative of at least 2 independent experiments.

induction in *Gpt1* and *Gpt2* mRNA, respectively (Figure 3D). Notably, *Gpt2* mRNA was induced later in the activation process, and its levels were significantly higher at 48 and 72 h post-activation compared to naive T cells (Figure S3C). Our recently published proteomic data showed a greater than 5-fold induction in protein levels of subunits in the PDH and LDH complexes during T cell activation (Ron-Harel et al., 2016), whereas GPT levels remained undetectable throughout (Figure S3D). Western blot analysis further verified that neither GPT1 nor GPT2 were induced during T cell activation (Figure 3E). Consistent with this observation, T cell activation in dFBS resulted in a decrease in cellular alanine pools (Figure 3F). Although GPT protein levels remain low even at 72 h post-activation, we detected some alanine synthesis from glucose at 24 h (Figure S3A) and saw a slight increase in cellular alanine concentrations over time in cells activated in dFBS (Figure 3F), possibly driven by the increase in cellular pyruvate pool size by 24 h post-activation (Figure S3E). These results suggest that during early activation, low alanine transaminase activity does not meet the cellular needs for alanine, and therefore, T cells depend on extracellular alanine pools for proper activation.

Extracellular Alanine Is Used for Protein Synthesis

In contrast to the small changes in alanine transaminase expression, we measured a large induction of some of the alanine transporters during T cell activation, supporting the observation that T cells depend on extracellular alanine. Alanine is classified as a neutral amino acid. Of the five neutral amino acid transporters, two were highly induced upon T cell activation based on an analysis of our T cell proteome dataset: SLC1A5 (also known as ASCT2) and sodium-dependent neutral amino acid transporter 1 (SNAT1) (Figure S3F). In T cells, ASCT2 mainly regulates glutamine uptake (Nakaya et al., 2014), whereas the net effect of SNAT1 deletion in human CD4⁺ T cells is reduced alanine uptake (Matheson et al., 2015). Therefore, we focused our validation on SNAT1 as the major mediator of alanine uptake in CD4⁺ T cells. SNAT1 expression and protein levels were highly induced with T cell activation (Figures S3G and S3H).

As T cell activation did not substantially engage in alanine catabolism, we hypothesized that T cells take up alanine by SNAT1 to support the large boost in protein synthesis that occurs upon T cell activation (Figure 2A). To validate the incorporation of extracellular alanine into proteins, naive T cells were activated *ex vivo* in dFBS media supplemented with [¹⁵N¹³C]-alanine. Cells were collected at different time points post-activation, followed by protein hydrolysis and analysis of protein-derived alanine by LC/MS (Figure 4A). Strikingly, the contribution of extracellular alanine to total protein remains low for the first 6 h, but by 24 h, over 50% of alanine in proteins was labeled. Furthermore, the labeled alanine was exclusively of the m+4 isotopomer, indicating direct incorporation of extracellular alanine (Figure 4B). Thus, extracellular alanine is taken up by T cells upon activation and is directly used for protein synthesis without metabolic interconversion by transamination.

To evaluate whether extracellular alanine is also needed for protein synthesis during the first 6 h of activation, we grew cells initially in dFBS, before adding back alanine. Statistically significant decreases in cell size were observed for any delay of 3 h

or more (Figures S3I and S3J). Thus, T cells require extracellular alanine, possibly for protein synthesis, after only a few hours post-activation.

To provide further evidence for the requirement of alanine for protein synthesis, we quantified the number of actively translating ribosomes, taking advantage of the fact that puromycin selectively binds to actively translating ribosomes, and its binding can be quantified using fluorescent anti-puromycin antibody (Argüello et al., 2018; Dadehbeigi and Dickson, 2013; Goodman and Hornberger, 2013) (Figure 4C). Our analysis demonstrated a reduction in active protein translation in T cells stimulated in media containing dFBS compared to cFBS and a complete rescue with alanine supplementation (Figures 4D and 4E). The specificity of the fluorescent signal was validated by the addition of harringtonine, an inhibitor of translation that disrupts ribosome-mRNA complexes. Treatment with harringtonine abolished the signal (Figure 4D).

Uncharged tRNAs activate GCN2 to inhibit translation (Harding et al., 2000; Pakos-Zebrucka et al., 2016). GCN2 induces expression of ATF4 that upregulates the expression of amino acid transporters and metabolic genes (Yang et al., 2018). To test whether this stress response is activated by alanine deprivation, naive CD4⁺ T cells were stimulated in media containing either cFBS, dFBS, or dFBS + alanine. Glutamine-deprived media and naive cells were used as positive and negative controls, respectively. Cells were collected 3 h post-activation and analyzed by western blot. ATF4 levels were induced in cells deprived of alanine (dFBS media) and completely reversed by alanine supplementation (Figure 4F). In sum, upon activation, naive T cells upregulate alanine uptake to fuel protein synthesis.

Alanine Depletion Inhibits Memory T Cell Restimulation

We further examined the role of alanine in supporting naive, activated, and memory CD8⁺ T cells. To this end, we used a well-established *in vivo* model of acute lymphocytic choriomeningitis virus (LCMV) infection (Figure 5A). Because our initial observations were made in naive CD4⁺ T cells, we first validated that naive CD8⁺ T cells were similarly dependent on extracellular alanine for initial activation. Naive CD8⁺ T cells were stimulated *ex vivo* with plate-bound anti-CD3/anti-CD28 in the indicated media conditions (Figure S4A). Stimulation-induced cell growth and proliferation were impaired in CD8⁺ T cells activated in dFBS media compared to cells activated in cFBS media and rescued by alanine supplementation (Figures S4B and S4C, respectively). CD8⁺ T cells, like CD4⁺ T cells, induced SNAT1 levels with activation (Figure S4D). Moreover, analysis by puromycin treatment (as described in Figure 4C) indicated reduced active translation in CD8⁺ T cells deprived of alanine and a complete rescue with alanine supplementation (Figure S4E).

Because T cells can eventually proliferate in dFBS (Figures 1D and 1J), we hypothesized that extracellular alanine would not be required for effector T cell function. To assess the need for extracellular alanine during antigen-specific T cell activation, P14 TCR transgenic CD8⁺ T cells specific for LCMV peptide GP₃₃₋₄₁ were transferred into wild-type C57BL/6 recipients and infected with LCMV Armstrong, which causes an acute viral infection. Splenocytes were harvested on day 8 after LCMV infection, during the effector phase of the immune response to LCMV, cultured

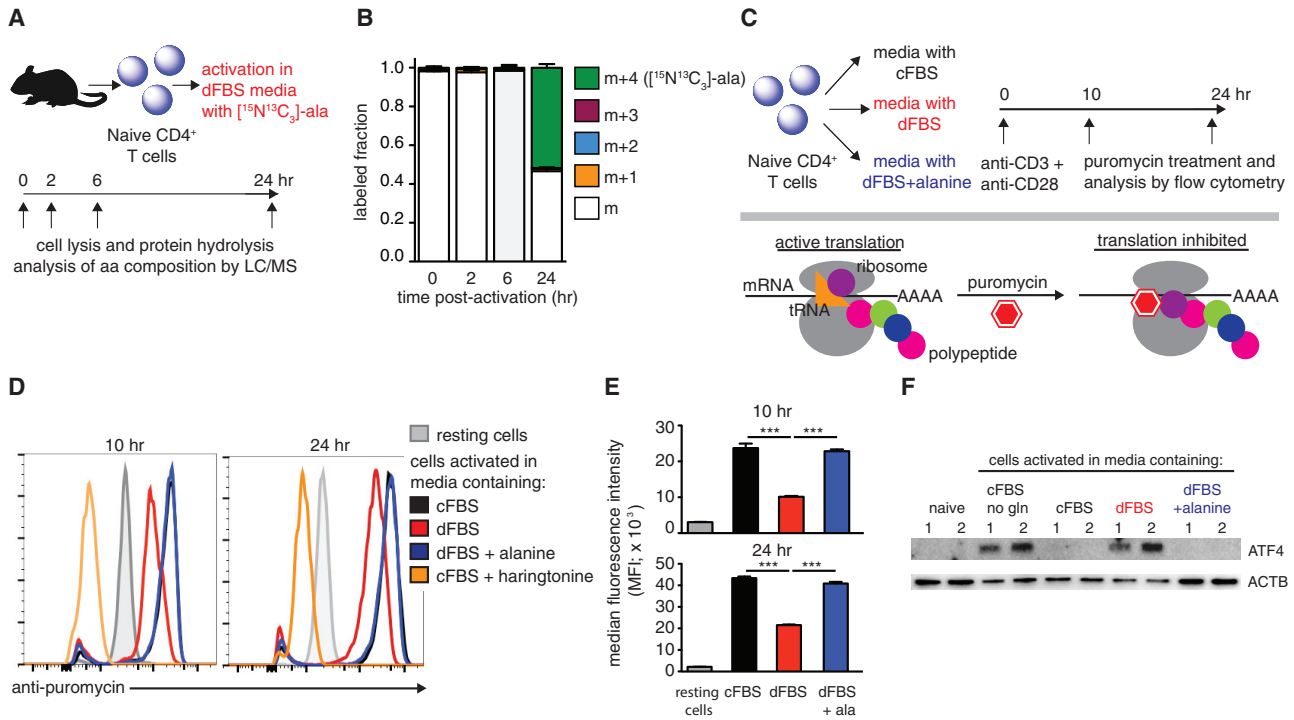


Figure 4. Alanine Deprivation Inhibits Activation-Induced Protein Synthesis

(A) Experimental design for measuring the incorporation of extracellular alanine into proteins during T cell activation.
 (B) Alanine-labeled fraction in total cell proteome of activated T cells ($n = 2$).
 (C) Experimental design to quantify active protein translation during T cell activation. Purified naive $CD4^+$ T cells were activated in different medium conditions and were treated with puromycin (binds active translation complexes) at 10 and 24 h, followed by flow cytometry analysis.
 (D) Representative flow cytometry plots of >3 experiments that measured active translation in the different conditions. T cells treated with harringtonine (to disrupt translation) serve as negative controls.
 (E) Quantitation of anti-puromycin median fluorescence intensity (MFI; $n = 3$).
 (F) Representative western blot images measuring ATF4 levels in naive T cells, and T cells activated for 3 h in the indicated medium conditions. Cells activated in glutamine-depleted media serve as a positive control.
 Results are representative of at least 3 independent experiments.

in vitro for 5 h in dFBS or cFBS media with GP_{33-41} LCMV peptide (Figure S5A), and effector functions assessed by flow cytometry (see Figure S5B for gating strategy). No significant differences were seen in the production of effector molecules granzyme B (GzB), $IFN\gamma$, and $TNF\alpha$ or proliferation (assessed by staining against Ki67) as a function of alanine availability (Figures S5C–S5F). Thus, once metabolically active, T cells do not depend on extracellular alanine.

Unlike active effector T cells, memory cells are metabolically quiescent. To explore their requirements for extracellular alanine, we analyzed splenocytes from LCMV-infected mice at day 30 post-infection (memory phase). The splenocytes were incubated *ex vivo* for 5 h under the indicated media conditions in the presence of the GP_{33-41} LCMV peptide (Figure 5A). Splenocytes were then stained and analyzed by flow cytometry to assess antigen-specific T cell responses. Restimulation of memory T cells under conditions of alanine deprivation (dFBS media) caused a significant reduction in the production of the proinflammatory cytokines $IFN\gamma$ and $TNF\alpha$. The inhibitory effect of alanine deprivation manifested as a reduced percentage of cytokine-expressing T cells (Figures 5B and 5D for $IFN\gamma$ and $TNF\alpha$, respec-

tively) and lower cytokine production per cell (Figures 5C and 5E for $IFN\gamma$ and $TNF\alpha$, respectively). The production of both cytokines was completely restored with alanine supplementation (Figures 5B–5E). Interestingly, GzB production was not negatively affected by alanine deprivation and was even slightly increased in dFBS media (Figures S5G and S5H), suggesting that GzB might be pre-formed and stored in the cells prior to restimulation. Proliferation rates, measured by staining against the endogenous marker Ki67, were low among the restimulated memory T cells under all media conditions (Figure 5F), potentially due to the short stimulation (5 h). Yet, a minor reduction in $Ki67^+$ cells was observed under alanine deprivation (Figure 5F). Thus, extracellular alanine is required for effector cytokine production by memory $CD8^+$ T cells upon restimulation.

DISCUSSION

In this study, we identify alanine as a semi-essential amino acid for T cells during activation. Extracellular alanine is needed early in the activation program (3–6 h) of both naive and memory T cells, and failure to meet this requirement leads to impaired

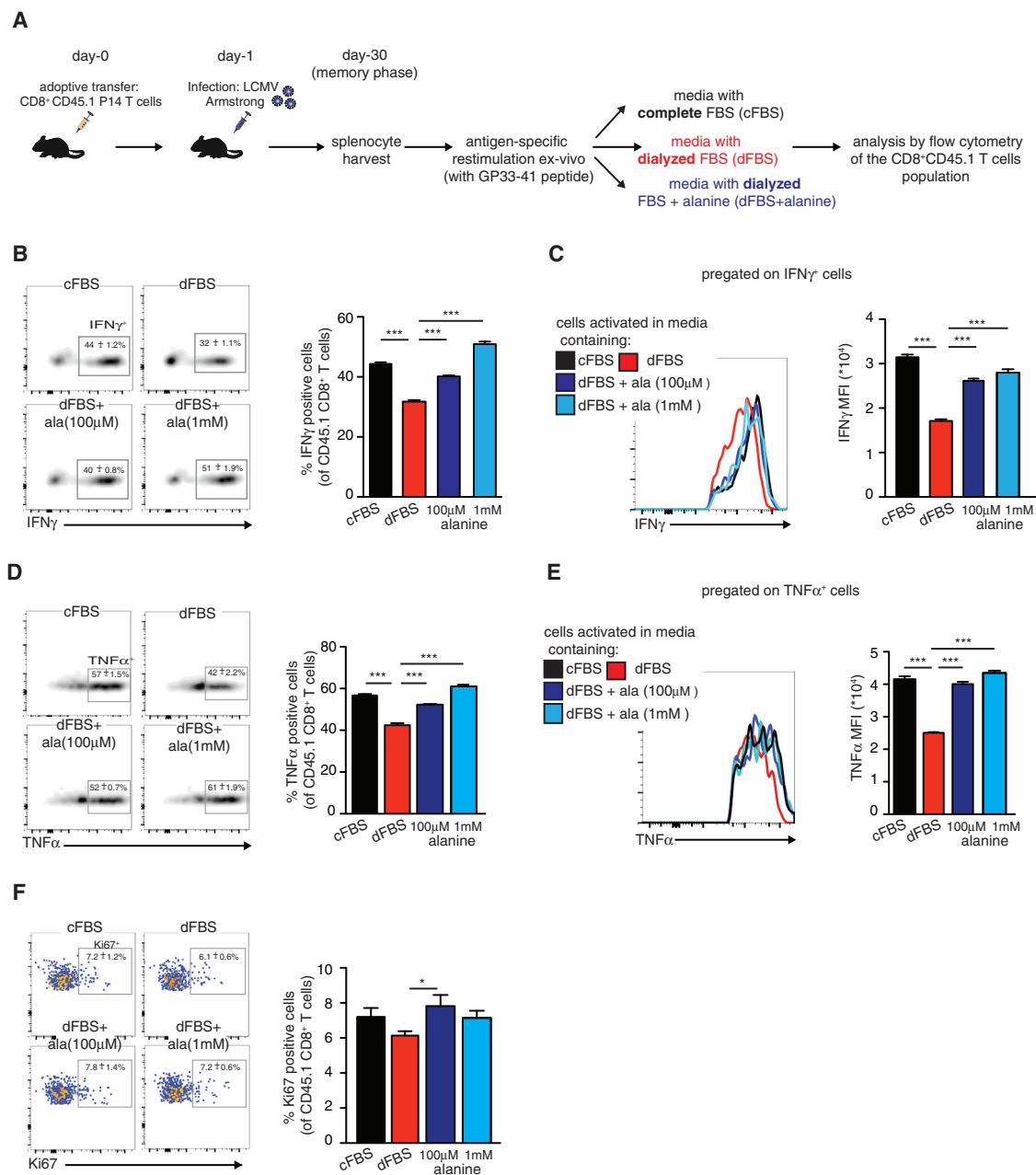


Figure 5. Extracellular Alanine Is Essential for Memory T Cell Restimulation

(A) Experimental design for assessing the need for extracellular alanine during memory T cell restimulation.

(B) Representative flow cytometry plots showing intracellular IFN γ staining following restimulation, and quantification of IFN γ -positive cells.

(C) Representative flow cytometry histograms and quantification of IFN γ MFI.

(D) Representative flow cytometry plots showing intracellular TNF α staining following restimulation and quantification of TNF α positive cells.

(E) Representative flow cytometry histograms and quantification of TNF α MFI.

(F) Representative flow cytometry plots showing intracellular Ki67 staining following restimulation, and quantification of Ki67-positive cells.

Representative plots of two independent experiments, n = 5 mice. Results are mean ± SEM. *p < 0.05, **p < 0.01, ***p < 0.001 (Student's t test comparing each of the conditions to dFBS media).

metabolic reprogramming, including reduced glucose uptake and decreased levels of metabolites in central carbon metabolism. This demand for extracellular alanine stems mainly from the requirement for alanine monomers for protein produc-

tion, as alanine taken up during T cell stimulation is not catabolized and is directly incorporated into proteins.

How does nutrient availability control T cell activation? T cell activation induces rapid cell growth and proliferation and

secretion of effector molecules. To fuel these biosynthetic and energy demands, T cells evolve to rely on the resources in their environment: activation signals induce expression of glucose and amino acid transporters as the cells require sustained uptake of nutrients (Rollings et al., 2018; Sinclair et al., 2013). Moreover, nutrient-sensitive signaling pathways such as mTOR, O-linked β -N-acetylglucosamine (O-GlcNAc), and cMYC regulate T cell activation and differentiation (Hukelmann et al., 2016; Sinclair et al., 2013; Swamy et al., 2016), thus connecting metabolite availability with function. Reliance on extracellular alanine joins other nutrient dependencies of activated T cells established in recent years, including glucose (Cham and Gajewski, 2005), glutamine (Nakaya et al., 2014), leucine (Ananieva et al., 2016), serine (Ma et al., 2017), and arginine (Geiger et al., 2016; Rodriguez et al., 2007). In all cases, restriction of the specific metabolite inhibited T cell activation and/or effector functions. Recent studies suggest that metabolic restriction helps cancer cells escape immune surveillance. Specifically, low glucose availability within the tumor microenvironment inhibits anti-tumor immunity (Chang et al., 2015).

Alanine is the second most abundant amino acid in the circulation, after glutamine, which makes it very accessible to T cells, especially those in organs with ample blood supply. Interestingly, an analysis of changes in the abundance of cell surface proteins during HIV infection of human CD4⁺ T cells identified a specific downregulation of SNAT1 on infected T cells and subsequent reduction of alanine uptake (Matheson et al., 2015). That study further suggested that alanine is catabolized by T cells and that downregulation of SNAT1 reduced glutamate pools. Similarly, a study in pancreatic cancer cells showed reliance on extracellular alanine as a source of carbon for the TCA cycle (Sousa et al., 2016). In our studies, we could not detect any evidence of alanine catabolism by T cells.

Our finding that T cells depend on extracellular pools of alanine is surprising, especially because alanine is a nonessential amino acid, for which mammalian cells possess the necessary synthetic machinery. Moreover, activated T cells are highly engaged in glycolysis and glutaminolysis, resulting in significant flux through pyruvate and glutamate, respectively, the immediate substrates for alanine production. Using estimated mammalian cell concentrations of pyruvate and glutamate under standard tissue culture conditions, we found that the production of alanine from pyruvate is thermodynamically favorable, with $\Delta G \sim -10$ KJ/mol by using the Weizmann equilibrium calculator (Flamholz et al., 2012; Park et al., 2016). This suggests that appreciable GPT expression during early activation would facilitate alanine production. Therefore, we speculate that GPT expression may be intentionally suppressed during T cell activation.

It is possible that T cells sacrifice the ability to produce alanine early in activation to avoid depleting cellular pyruvate pools, which may be more critical for fueling the mitochondrial biosynthetic program (Buck et al., 2017; Ron-Harel et al., 2016) and/or for accepting electrons from NADH to allow regeneration of NAD⁺. In this respect, it is important to note that glycolysis induces flux through pyruvate without increasing net pyruvate. The production of pyruvate requires a transfer of electrons

from NADH into the mitochondrion and ultimately to molecular oxygen. Although an efficient source of ATP, this process can bottleneck due to low oxygen availability (as can occur in ischemic infection sites or tumors) or inefficient machinery for electron transfer from the cytosol to mitochondrion (as may occur early in T cell activation, when mitochondria are relatively scarce). Indeed, increasing evidence identifies oxidized carbon as a limiting reagent in multiple cellular contexts (Birsoy et al., 2015; Gui et al., 2016). By taking in exogenous alanine, T cells may conserve oxidized carbon for more pressing needs, including synthesis of aspartate, the amino acid that is least abundant in the circulation.

In sum, we find that access to extracellular alanine is essential during early T cell activation and memory T cell restimulation to fuel protein synthesis. Serum alanine concentrations are known to fluctuate in mammals by as much as 2- to 3-fold depending on the fed-state, dietary composition, and feeding schedule for the animal (Knipfel et al., 1972; Krebs, 1972). The local concentrations of alanine in different tissue niches have not been thoroughly annotated. Moreover, alanine is depleted in some tumors (Kamphorst et al., 2015). It is possible that the control of local alanine levels through the uptake or secretion of alanine by resident cells in the lymphatic tissue, or other tissues where resident memory T cells get re-activated (such as the skin, the lungs, or the brain), may impact T cell activation. Similarly, alanine availability in tumors may affect anti-tumor immunity. Taken together, our findings suggest that T cells may be sensitive to changing alanine concentrations during physiological or disease states. Thus, interventions that target alanine uptake may provide a therapeutic strategy for modulating T cell activation or memory function.

STAR★METHODS

Detailed methods are provided in the online version of this paper and include the following:

- KEY RESOURCES TABLE
- LEAD CONTACT AND MATERIALS AVAILABILITY
- EXPERIMENTAL MODEL AND SUBJECT DETAILS
 - Mice
- METHOD DETAILS
 - Culture and stimulation of naive CD4⁺ T cells
 - Metabolite measurements by LC-MS
 - Isolation of protein and hydrolysis into amino acid monomers
 - LCMV infection and *ex vivo* stimulation of effector and memory T cells
 - Flow cytometry
 - Glucose uptake
 - Real-time PCR
 - Protein content analysis by western blot
 - Mitochondrial respiration and glycolysis
 - Analysis of active protein synthesis with puromycin treatment
- QUANTIFICATION AND STATISTICAL ANALYSIS
 - Statistical analysis
- DATA AND CODE AVAILABILITY

SUPPLEMENTAL INFORMATION

Supplemental Information can be found online at <https://doi.org/10.1016/j.celrep.2019.08.034>.

ACKNOWLEDGMENTS

The authors thank Matthew Coxe for his help with performing experiments. This study was supported by grants from the Ludwig Center at Harvard Medical School; NIH grants U54-CA225088 (A.H.S. and M.C.H.) and R01CA213062 (M.C.H.); and by NSF Graduate Research Fellowship Program (G.N.). N.R.-H. was supported by The European Molecular Biology Organization long-term postdoctoral fellowship and the Israeli National Postdoctoral Award Program for Advancing Women In Science.

AUTHOR CONTRIBUTIONS

Conceptualization, N.R.-H., J.M.G., A.H.S., J.D.R., and M.C.H.; Methodology, N.R.-H., J.M.G., G.N., M.W.L., A.H.S., J.D.R., and M.C.H.; Investigation, N.R.-H., J.M.G., G.N., M.W.L., and Y.T.; Writing-Original Draft, N.R.-H., J.M.G., J.D.R., and M.C.H.; Writing-Review & Editing, N.R.-H., J.M.G., G.N., M.W.L., A.H.S., J.D.R., and M.C.H.; Visualization, N.R.-H., J.M.G., G.N., A.H.S., J.D.R., and M.C.H.; Funding Acquisition, A.H.S., J.D.R., and M.C.H.

DECLARATION OF INTERESTS

The authors declare no competing interests.

Received: December 11, 2018

Revised: April 15, 2019

Accepted: August 9, 2019

Published: September 17, 2019

REFERENCES

- Ananieva, E.A., Powell, J.D., and Hutson, S.M. (2016). Leucine Metabolism in T Cell Activation: mTOR Signaling and Beyond. *Adv. Nutr.* *7*, 798S–805S.
- Argüello, R.J., Reverendo, M., Mendes, A., Camosseto, V., Torres, A.G., Ribas de Pouplana, L., van de Pavert, S.A., Gatti, E., and Pierre, P. (2018). SunRISE—measuring translation elongation at single-cell resolution by means of flow cytometry. *J. Cell Sci.* *131*, jcs214346.
- Berod, L., Friedrich, C., Nandan, A., Freitag, J., Hagemann, S., Harmrolfs, K., Sandouk, A., Hesse, C., Castro, C.N., Bähre, H., et al. (2014). De novo fatty acid synthesis controls the fate between regulatory T and T helper 17 cells. *Nat. Med.* *20*, 1327–1333.
- Birsoy, K., Wang, T., Chen, W.W., Freinkman, E., Abu-Remaileh, M., and Sabatini, D.M. (2015). An Essential Role of the Mitochondrial Electron Transport Chain in Cell Proliferation Is to Enable Aspartate Synthesis. *Cell* *162*, 540–551.
- Buck, M.D., Sowell, R.T., Kaech, S.M., and Pearce, E.L. (2017). Metabolic Instruction of Immunity. *Cell* *169*, 570–586.
- Carr, E.L., Kelman, A., Wu, G.S., Gopaul, R., Senkevitch, E., Aghvanyan, A., Turay, A.M., and Frauwirth, K.A. (2010). Glutamine uptake and metabolism are coordinately regulated by ERK/MAPK during T lymphocyte activation. *J. Immunol.* *185*, 1037–1044.
- Cham, C.M., and Gajewski, T.F. (2005). Glucose availability regulates IFN- γ production and p70S6 kinase activation in CD8⁺ effector T cells. *J. Immunol.* *174*, 4670–4677.
- Chang, C.H., Qiu, J., O'Sullivan, D., Buck, M.D., Noguchi, T., Curtis, J.D., Chen, Q., Gindin, M., Gubin, M.M., van der Windt, G.J., et al. (2015). Metabolic Competition in the Tumor Microenvironment Is a Driver of Cancer Progression. *Cell* *162*, 1229–1241.
- Clasquin, M.F., Melamud, E., and Rabinowitz, J.D. (2012). LC-MS data processing with MAVEN: a metabolomic analysis and visualization engine. *Curr. Protoc. Bioinformatics Chapter 14*, Unit14 11.
- Dadehbeigi, N., and Dickson, A.J. (2013). Application of a nonradioactive method of measuring protein synthesis in industrially relevant Chinese hamster ovary cells. *Biotechnol. Prog.* *29*, 1043–1049.
- Flamholz, A., Noor, E., Bar-Even, A., and Milo, R. (2012). eQuilibrator—the biochemical thermodynamics calculator. *Nucleic Acids Res.* *40*, D770–D775.
- Geiger, R., Rieckmann, J.C., Wolf, T., Basso, C., Feng, Y., Fuhrer, T., Koga-deeva, M., Picotti, P., Meissner, F., Mann, M., et al. (2016). L-Arginine Modulates T Cell Metabolism and Enhances Survival and Anti-tumor Activity. *Cell* *167*, 829–842.e813.
- Goodman, C.A., and Hornberger, T.A. (2013). Measuring protein synthesis with SUNSET: a valid alternative to traditional techniques? *Exerc. Sport Sci. Rev.* *41*, 107–115.
- Gui, D.Y., Sullivan, L.B., Luengo, A., Hosios, A.M., Bush, L.N., Gitego, N., Davidson, S.M., Freinkman, E., Thomas, C.J., and Vander Heiden, M.G. (2016). Environment Dictates Dependence on Mitochondrial Complex I for NAD⁺ and Aspartate Production and Determines Cancer Cell Sensitivity to Metformin. *Cell Metab.* *24*, 716–727.
- Harding, H.P., Novoa, I., Zhang, Y., Zeng, H., Wek, R., Schapira, M., and Ron, D. (2000). Regulated translation initiation controls stress-induced gene expression in mammalian cells. *Mol. Cell* *6*, 1099–1108.
- Hukelmann, J.L., Anderson, K.E., Sinclair, L.V., Grzes, K.M., Murillo, A.B., Hawkins, P.T., Stephens, L.R., Lamond, A.I., and Cantrell, D.A. (2016). The cytotoxic T cell proteome and its shaping by the kinase mTOR. *Nat. Immunol.* *17*, 104–112.
- Kamphorst, J.J., Nofal, M., Comisso, C., Hackett, S.R., Lu, W., Grabocka, E., Vander Heiden, M.G., Miller, G., Drebin, J.A., Bar-Sagi, D., et al. (2015). Human pancreatic cancer tumors are nutrient poor and tumor cells actively scavenge extracellular protein. *Cancer Res.* *75*, 544–553.
- Knipfel, J.E., Keith, M.O., Christensen, D.A., and Owen, B.D. (1972). Diet and feeding interval effects on serum amino acid concentrations of growing swine. *Can. J. Anim. Sci.* *52*, 143–153.
- Krebs, H.A. (1972). Some aspects of the regulation of fuel supply in omnivorous animals. *Adv. Enzyme Regul.* *10*, 397–420.
- Ma, E.H., Bantug, G., Griss, T., Condotta, S., Johnson, R.M., Samborska, B., Mainolfi, N., Suri, V., Guak, H., Balmer, M.L., et al. (2017). Serine Is an Essential Metabolite for Effector T Cell Expansion. *Cell Metab.* *25*, 482.
- Matheson, N.J., Sumner, J., Wals, K., Rapiteanu, R., Weekes, M.P., Vigan, R., Weinelt, J., Schindler, M., Antrobus, R., Costa, A.S., et al. (2015). Cell Surface Proteomic Map of HIV Infection Reveals Antagonism of Amino Acid Metabolism by Vpu and Nef. *Cell Host Microbe* *18*, 409–423.
- Nakaya, M., Xiao, Y., Zhou, X., Chang, J.H., Chang, M., Cheng, X., Blonska, M., Lin, X., and Sun, S.C. (2014). Inflammatory T cell responses rely on amino acid transporter ASCT2 facilitation of glutamine uptake and mTORC1 kinase activation. *Immunity* *40*, 692–705.
- Pakos-Zebrucka, K., Koryga, I., Mnich, K., Ljujic, M., Samali, A., and Gorman, A.M. (2016). The integrated stress response. *EMBO Rep.* *17*, 1374–1395.
- Park, J.O., Rubin, S.A., Xu, Y.F., Amador-Noguez, D., Fan, J., Shlomi, T., and Rabinowitz, J.D. (2016). Metabolite concentrations, fluxes and free energies imply efficient enzyme usage. *Nat. Chem. Biol.* *12*, 482–489.
- Patsoukis, N., Bardhan, K., Chatterjee, P., Sari, D., Liu, B., Bell, L.N., Karoly, E.D., Freeman, G.J., Petkova, V., Seth, P., et al. (2015). PD-1 alters T-cell metabolic reprogramming by inhibiting glycolysis and promoting lipolysis and fatty acid oxidation. *Nat. Commun.* *6*, 6692.
- Ramsay, G., and Cantrell, D. (2015). Environmental and metabolic sensors that control T cell biology. *Front. Immunol.* *6*, 99.
- Rodriguez, P.C., Quiceno, D.G., and Ochoa, A.C. (2007). L-arginine availability regulates T-lymphocyte cell-cycle progression. *Blood* *109*, 1568–1573.
- Rollings, C.M., Sinclair, L.V., Brady, H.J.M., Cantrell, D.A., and Ross, S.H. (2018). Interleukin-2 shapes the cytotoxic T cell proteome and immune environment-sensing programs. *Sci. Signal.* *11*, eaap8112.

- Ron-Harel, N., Santos, D., Ghergurovich, J.M., Sage, P.T., Reddy, A., Lovitch, S.B., Dephoure, N., Satterstrom, F.K., Sheffer, M., Spinelli, J.B., et al. (2016). Mitochondrial Biogenesis and Proteome Remodeling Promote One-Carbon Metabolism for T Cell Activation. *Cell Metab.* *24*, 104–117.
- Rotter, V., Yakir, Y., and Trainin, N. (1979). Role of L-alanine in the response of human lymphocytes to PHA and Con A. *J. Immunol.* *123*, 1726–1731.
- Sinclair, L.V., Rolf, J., Emslie, E., Shi, Y.B., Taylor, P.M., and Cantrell, D.A. (2013). Control of amino-acid transport by antigen receptors coordinates the metabolic reprogramming essential for T cell differentiation. *Nat. Immunol.* *14*, 500–508.
- Sousa, C.M., Biancur, D.E., Wang, X., Halbrook, C.J., Sherman, M.H., Zhang, L., Kremer, D., Hwang, R.F., Witkiewicz, A.K., Ying, H., et al. (2016). Pancreatic stellate cells support tumour metabolism through autophagic alanine secretion. *Nature* *536*, 479–483.
- Su, X., Lu, W., and Rabinowitz, J.D. (2017). Metabolite Spectral Accuracy on Orbitraps. *Anal. Chem.* *89*, 5940–5948.
- Swamy, M., Pathak, S., Grzes, K.M., Damerow, S., Sinclair, L.V., van Aalten, D.M., and Cantrell, D.A. (2016). Glucose and glutamine fuel protein O-GlcNAcylation to control T cell self-renewal and malignancy. *Nat. Immunol.* *17*, 712–720.
- Tsugita, A., and Scheffler, J.J. (1982). A rapid method for acid hydrolysis of protein with a mixture of trifluoroacetic acid and hydrochloric acid. *Eur. J. Biochem.* *124*, 585–588.
- Wieman, H.L., Wofford, J.A., and Rathmell, J.C. (2007). Cytokine stimulation promotes glucose uptake via phosphatidylinositol-3 kinase/Akt regulation of Glut1 activity and trafficking. *Mol. Biol. Cell* *18*, 1437–1446.
- Wofford, J.A., Wieman, H.L., Jacobs, S.R., Zhao, Y., and Rathmell, J.C. (2008). IL-7 promotes Glut1 trafficking and glucose uptake via STAT5-mediated activation of Akt to support T-cell survival. *Blood* *111*, 2101–2111.
- Yang, X., Xia, R., Yue, C., Zhai, W., Du, W., Yang, Q., Cao, H., Chen, X., Obando, D., Zhu, Y., et al. (2018). ATF4 Regulates CD4⁺ T Cell Immune Responses through Metabolic Reprogramming. *Cell Rep.* *23*, 1754–1766.

STAR★METHODS

KEY RESOURCES TABLE

REAGENT or RESOURCE	SOURCE	IDENTIFIER
Antibodies		
Anti-mouse CD3e (145-2C11)	BioXCell	BE0001-1
Anti-mouse CD28 (37.51)	BioXCell	BE0015-1
APC/cy7 anti-mouse CD8b (YTS156.7.7)	Biolegend	126619
PE anti-mouse CD45.1 (H1.2F3)	Biolegend	110707
PerCP/cy5.5 anti-mouse CD69 (H1.2F3)	Biolegend	104521
APC anti-mouse IFN γ (XMG1.2)	Biolegend	505809
FITC anti-mouse GzB (GB11)	Biolegend	515403
PerCP/cy5.5 anti-mouse TNF α (MP6-XT22)	Biolegend	506321
PerCP/cy5.5 anti-mouse Ki67 (16A8)	Biolegend	652423
BV421 donkey anti-rabbit IgG (Poly4064)	Biolegend	406410
Rabbit anti-GPT1	Proteintech	16897-1-AP
Rabbit anti-GPT2	Proteintech	16757-1-AP
Rabbit anti-ATF4 (D4B8)	Proteintech	11815
Rabbit anti-SNAT1 (D9L2P)	Cell Signaling	36057
Rabbit anti-ACTB	Sigma Aldrich	A2066
HRP conjugated rabbit anti-ACTB (13EB)	Cell signaling	5125
AF604 anti-puromycin	EMD Millipore Corp	MABE343-AF647
Chemicals, Peptides, and Recombinant Proteins		
L-Alanine	Sigma Aldrich	A7627-100G
¹⁵ N labeled alanine	Cambridge Isotope Laboratories, Inc.	NLM-454
³ - ¹³ C labeled pyruvate	Cambridge Isotope Laboratories, Inc.	CLM-1575
U- ¹³ C- ¹⁵ N glutamine	Cambridge Isotope Laboratories, Inc.	CNLM-1275
RPMI 1640	Thermo Fisher	11875-119
RPMI 1640 (no glutamine)	Thermo Fisher	21870100
FBS	Corning	45000-734
Dialyzed FBS (1698218, 1743489)	Thermo Fisher	26400044
Oligomycin A	Sigma Aldrich	75351
FCCP	Sigma Aldrich	C2920
Rotenone	Sigma Aldrich	R8875
Antimycin A	Sigma Aldrich	A8674
2-NBDG	Thermo Fisher	N13195
Puromycin	InvivoGen	ant-pr-1
CellTrace violet	Thermo Fisher	C34557
Golgi stop	BD Biosciences	554724
Complete Mini Protease Inhibitor	Roche	11873580001
Recombinant IL-7	R&D systems	407-ML
Critical Commercial Assays		
CD4 (L3T4) Microbeads, mouse	Miltenyi Biotec	130-117-043
CD8 (Ly-2) Microbeads, mouse	Miltenyi Biotec	130-117-044
Foxp3/transcription factor staining buffer set	eBioscience	00-5523-00
Th1/Th2/Th17 cytometric bead array, mouse	BD Biosciences	560485
iScript cDNA synthesis kit	BioRad	1708891
DNeasy blood and tissue kit	QIAGEN	69506

(Continued on next page)

Continued		
REAGENT or RESOURCE	SOURCE	IDENTIFIER
Experimental Models: Organisms/Strains		
C57BL/6J	The Jackson Laboratory	000664
B6.Cg-Tcra ^{tm1Mom} Tg(TcrLCMV)327Sdz/TacMmjax	The Jackson Laboratory	37394-JAX
B6.SJL-Ptprc ^a Pepc ^b /BoyJ	The Jackson Laboratory	002014
Oligonucleotides		
Primer Snat1, F: TGAGACTGCCCAAATGCCTAAGGA, R: TCTCTGTTGCAGAAAGCTGGTGGGA	This paper	N/A
Primer Pdha, F: CCACCTCATCACTGCCTATC, R: CCTTAGCACAAACCTCCTCTT	This paper	N/A
Primer Ldha, F: ACAAACTCAAGGGCGAGATG, R: GGAGTTCGCAGTTACACAGTAG	This paper	N/A
Primer Gpt1, F: GGAAGGTGCTAACTCTGGATAC, R: GGCACGGATAACCTCAGTAAA	This paper	N/A
Primer Gpt2, F: AACTGTATCCGTGAAGATGTGGC, R: CAGGTAAATGTTGTCTGGGTCTG	This paper	N/A
Software and Algorithms		
Prism	GraphPad Sofwate	https://www.graphpad.com/scientific-software/prism/
FlowJo	FlowJo	https://www.flowjo.com
MAVEN software suite	Clasquin et al., 2012	https://maven.apache.org

LEAD CONTACT AND MATERIALS AVAILABILITY

This study did not generate new reagents. Further information and requests for resources and reagents should be directed to and will be fulfilled by the Lead Contact, Marcia Haigis (marcia_haigis@hms.harvard.edu).

EXPERIMENTAL MODEL AND SUBJECT DETAILS

Mice

Wild-type C57BL/6 mice were purchased from the Jackson Laboratory (Bar Harbor, ME). P14 (Taconic B6.Cg-Tcra^{tm1Mom} Tg(TcrLCMV)327Sdz) were backcrossed 10 generations to Jackson C57BL/6J and crossed to the CD45.1 congenic background (B6.SJL-Ptprca Pepc^b/BoyJ). 7-10-week-old female mice were used for all experiments. Mice were housed in specific pathogen-free conditions at Harvard Medical School and used in accordance with animal care guidelines from the Harvard Medical School Standing Committee on Animals and the National Institutes of Health.

METHOD DETAILS

Culture and stimulation of naive CD4⁺ T cells

Naive CD4⁺CD62L^{hi}CD44^{lo}CD25⁻ or CD8⁺CD62L^{hi}CD44^{lo}CD25⁻ cells were purified from splenocytes using CD4⁺ or CD8⁺ magnetic beads (Miltenyi Biotec) and sorted by flow cytometry (purity > 99%) as previously described ([Ron-Harel et al., 2016](#)). Naive T cells were cultured at 37°C and 5% CO₂ in complete RPMI media (RPMI, supplemented with 10% FBS, 10 mM HEPES, 10 U/ml penicillin/streptomycin, and 50 μM 2-mercaptoethanol (all from Life Technologies)). When indicated, dialyzed FBS was used in combination or as a replacement of standard FBS, and alanine (Sigma Aldrich), isotopically labeled alanine (Cambridge Isotope Laboratories, Inc.) or isotopically labeled pyruvate (Cambridge Isotope Laboratories, Inc.) was added to achieve the denoted concentrations. For glutamine labeling experiments, glutamine-free RPMI (GIBCO) was supplemented with [U-¹³C,¹⁵N]-Glutamine (2 mM, Cambridge Isotope Laboratories, Inc.). Cells were activated *in vitro* with 4 μg/mL plate-bound anti-CD3 (clone 145-2C11; BioXCell) and anti-CD28 (clone 37.51; BioXCell), or co-cultured with antigen presenting cells (splenocytes that were depleted of T cells using anti-CD4 and anti-CD8 magnetic beads (Miltenyi Biotec.), with 2 μg/mL soluble anti-CD3. 50K T cells were incubated with 250K APCs per well, in a 96 well plate. In some experiments, IL-7 (5 ng/mL; R&D Systems) was added to culture media. In metabolite rescue experiments, media containing 10% dFBS was supplemented with denoted metabolites (achieving a final concentration of 100 μM, which was chosen to exceed the likely concentrations of these metabolites in media prepared with 10% cFBS, based on reported estimates of these metabolites in serum). Identical results were obtained when supplementing dFBS media with 10 μM of the same metabolites, except for alanine, which failed to rescue T cell activation at this concentration.

Metabolite measurements by LC-MS

For analysis of intracellular metabolites by liquid chromatography mass spectrometry, activated CD4⁺ T cells were collected into Eppendorf tubes, centrifuged at 9,500 g for 20 s at room temperature, resuspended in 1 mL PBS, and promptly centrifuged again under the same conditions. The supernatant was quickly removed and the pellets were extracted with 50–100 μ L extraction buffer (either 80% methanol/ 20% water or 40% acetonitrile/40% methanol/20% water + 0.5% formic acid). Total time from perturbation of the cells to quenching was \sim 1 min. Samples extracted w/ formic acid buffer were incubated 5 min on ice following by pH neutralization with 15% w/v ammonium hydroxide. Samples were stored at -80°C , followed by centrifugation at 4°C (\sim 15,000 g) to remove insoluble cell components. For serum and media metabolite analysis, 10 μ L of sample was diluted into 40 μ L of methanol cooled on dry ice. The mixture was centrifuged at 17,000 g for 5 min at 4°C , and the resulting supernatants were diluted and analyzed directly by LC-MS. For experiments where absolute metabolite concentrations were obtained, isotopically labeled internal standards were added to the extraction buffer.

Metabolites were analyzed using a quadrupole-orbitrap mass spectrometer (Q Exactive Plus, Thermo Fisher Scientific, Waltham, MA), coupled to hydrophilic interaction chromatography (HILIC) with LC separation on a XBridge BEH Amide column, or a stand-alone orbitrap (Thermo-Fisher Exactive) coupled to reversed-phase ion-pairing chromatography with LC separation on a Waters column. Both mass spectrometers were operating in negative ion mode and were coupled to their respective liquid chromatography methods via electrospray-ionization. Data were analyzed using the MAVEN software suite (Clasquin et al., 2012). Metabolite abundances were normalized to cell count. Unless otherwise indicated, isotopic labeling of metabolites arising from incubation with ^{13}C or ^{15}N labeled nutrients were corrected for natural abundance, as previously described (Su et al., 2017).

Isolation of protein and hydrolysis into amino acid monomers

Cell pellets were mixed in 200 μ L of lysis buffer (2% SDS, 150mM NaCl, 50mM Tris (pH 8.5), proteinase inhibitor mix (Roche, South San Francisco, CA, USA), 5mM DTT, and incubated on ice for 10 min, followed by incubation at 60°C for 45 min. Samples were allowed to cool to room temperature and incubated for 45 min with iodoacetamide to a final concentration of 14 mM. Samples were mixed with 3 parts ice-cold methanol, 1 part chloroform and 2.5 parts H₂O, and centrifuged at 4000 g for 10 min. Following removal of the top layer, 3 parts of ice-cold methanol were added, followed by centrifugation at 4000 g for 5 min. Following removal of the top layer, the samples were mixed with 3 parts of ice-cold acetone, vortexed, and centrifuged at 4000 g for 5 min. The pellet was then washed one more time in 2 mL ice-cold acetone, and stored at (-80°C) prior to chemical hydrolysis. The resulting protein pellet was resuspended in 6 N HCl/acetic acid (50:50, 100 μ L) and was heated at 95°C for one hour, using a slightly modified version of a reported protocol for protein hydrolysis (Tsugita and Scheffler, 1982). The resulting aqueous solution was diluted into 40% acetonitrile/40% methanol/20% water and analyzed by LC-MS.

LCMV infection and ex vivo stimulation of effector and memory T cells

Spleens were isolated from P14 TCR transgenic mice and naive CD8⁺ T cells were purified using the naive CD8⁺ MACS kit (> 95% purity; Miltenyi Biotec). Cells were transferred intravenously (500 cells) to C57BL/6 wild-type mice on day 0. The following day (day 1), the mice were intraperitoneally infected with 2×10^5 PFU LCMV Armstrong, and sacrificed at day 8 or 30 post infection for analysis. Spleens were isolated from LCMV-infected mice, dissociated, and ACK-lysed to remove red blood cells. Two million cells/well were plated in a 96 U bottom plate and incubated at 37°C for 4 hr with Golgi Stop (BD Biosciences) at 0.06% and LCMV GP₃₃₋₄₁ peptide at 1 μ g/mL. Cells were then harvested and processed for analysis by flow cytometry.

Flow cytometry

In vitro activated cells or cells isolated from LCMV-infected mice were collected, resuspended in staining buffer (PBS containing 1% fetal bovine serum and 2 mM EDTA), and stained directly with labeled antibodies from Biolegend against CD8 (YTS156.7.7), CD45.1 (A20), and CD69 (H1.2F3). For intracellular staining, the FoxP3 fix/perm kit (eBioscience) was used after surface staining, followed by staining against: IFN γ (XMG1.2), GzB (GB11), TNF α (MP6-XT22) and Ki67 (16A8). For assessment of proliferation, cells were loaded with CellTrace violet (Molecular Probes), according to the manufacturer's protocol. Analysis of cytokine levels in growth media was performed using the Th1/Th2/Th17 cytometric bead array (BD Biosciences), following the manufacturer's protocol. All flow cytometry was analyzed with an LSRII (BD biosciences) using standard filter sets, and FlowJo software (TreeStar).

Glucose uptake

Naive CD4⁺ T cells were activated with anti-CD3/CD28 antibodies in complete RPMI media supplemented with either 10% dialyzed FBS or 10% complete FBS. After 24 hours, cells were washed and starved of glucose by incubation in glucose-free, serum-free RPMI media for 30 minutes before incubation with 50 μ g/mL 2-deoxy-2-[(7-nitro-2,1,3-benzoxadiazol-4-yl)amino]-d-glucose (2-NBDG) for 20 min. Uptake was measured by flow cytometric evaluation of signal in the FITC channel. Fluorescence intensity was normalized to cell size, using the forward-side scatter.

Real-time PCR

Total DNA was isolated using DNeasy kit (QIAGEN). cDNA was synthesized using the iSCRIPT kit (BioRad). Quantitative PCR analysis was performed with SYBR green, using a LightCycler 480 (Roche). Primers used: Snat1: F: 5'- TGAGACTGCCCAAATGCCT AAGGA-3', R: 5'- TCTCTGTTGCAGAAAGCTGGTGGG –3'; Pdha: F: 5'- CCACCTCATCACTGCCTATC-3', R: 5'- CCTTTAGCA CAACCTCCTCTT-3'; Ldha: F: 5'-ACAAACTCAAGGGCGAGATG-3, R: 5'- GGAGTTCGCAGTTACACAGTAG-3; Gpt1: 5'- GGAAGG TGCTAACTCTGGATAC-3', R: 5'- GGCACGGATAACCTCAGTAAA-3'; Gpt2: F: 5'-AACTGTATCCGTGAAGATGTGGC-3', R: 5'-CA GGTAATGTTGTCTGGGTCTG-3';

Protein content analysis by western blot

Cells were lysed in lysis buffer (150 mM NaCl, 50 mM Tris-HCl, pH 7.5 and 0.5% NP-40) supplemented with protease inhibitor cocktail (Roche). Lysates were mixed with sample buffer (Tris-HCL pH 6.8, 30% glycerol, 10% SDS, 0.012% bromophenol blue) under reducing conditions, separated by sodium dodecyl sulfate polyacrylamide gel electrophoresis, and transferred to nitrocellulose membrane. The membranes were incubated for 1 hr in Tris-Buffered Saline (TBS) containing 0.1% Tween-20 and 5% nonfat milk, followed by an overnight incubation with the respective primary antibodies at 4°C. The membranes were then washed and incubated with horseradish peroxidase-conjugated secondary antibody for 1 hr, washed and developed using an enhanced chemiluminescence reagent (Thermo Scientific). Primary antibodies used: rabbit anti-GPT1 (16897-1-AP, Proteintech), rabbit anti-GPT2 (16757-1-AP, Proteintech), rabbit anti-ATF4 (D4B8, #11815, Cell Signaling), rabbit anti-SNAT1 (D9L2P, #36057, Cell Signaling), rabbit anti-ACTB (A2066, Sigma-Aldrich), HRP conjugated rabbit anti-ACTB (13E5, Cell Signaling).

Mitochondrial respiration and glycolysis

Oxygen consumption rate and extracellular acidification rate were measured from cells in non-buffered DMEM containing 5 mM glucose, 2 mM L-glutamine, and 1 mM sodium pyruvate, under basal conditions and in response to mitochondrial inhibitors: 1 μ M oligomycin, 1 μ M FCCP, 100 nM rotenone, and 1 μ M antimycin A (All from Sigma) on the XF96 Extracellular Flux Analyzer (Agilent Technologies).

Analysis of active protein synthesis with puromycin treatment

T cells were activated *in vitro* for up to 24 hr at the indicated times, puromycin (10 μ g/mL) was added to the culture for 10 min at 37°C. Some cells were treated with harringtonine (1 μ g/mL) for 15 min at 37°C, prior to addition of puromycin. Cells were then washed with cold PBS, processed for intracellular staining of puromycin (AF604 anti-puromycin, EMD Millipore Corp), and immediately analyzed by flow cytometry.

QUANTIFICATION AND STATISTICAL ANALYSIS

Statistical analysis

All statistical analyses were performed using Prism (Graphpad Software). We used unpaired Student's t test when comparing two groups, and one-way analysis of variance (ANOVA) followed by Tukey-Kramer's post hoc analysis, when comparing 3 groups.

DATA AND CODE AVAILABILITY

The proteomics dataset used in this study is available at [Ron-Harel et al. \(2016\)](#). All used software is available and listed in the [Key Resources Table](#). This study did not generate code or new datasets.